12-2011

Production and Fate of Transparent Exopolymer Particles in the Ocean

Oliver Wurl
Old Dominion University

Lisa Miller

Svein Vagle

Original Publication Citation

Wurl, O., Miller, L., & Vagle, S. (2011). Production and fate of transparent exopolymer particles in the ocean. *Journal of Geophysical Research: Oceans, 116,* C00H13. doi:10.1029/2011jc007342

Production and fate of transparent exopolymer particles in the ocean

Oliver Wurl,[1,2] Lisa Miller,[1] and Svein Vagle[1]

Received 6 June 2011; revised 26 September 2011; accepted 17 October 2011; published 30 December 2011.

[1] The production and fate of transparent exopolymer particles (TEP) have been investigated in various oceanic regions (tropical, temperate, and polar), from the sea surface microlayer (SML) to the deep ocean. Accumulation of TEP within the mixed layer was observed even in the absence of phytoplankton blooms, indicating abiotic processes are important in TEP production. The abiotic TEP aggregation rates measured in the tropical and temperate North Pacific and the Arctic Ocean averaged between 8 and 12 μmol C L^{-1} d^{-1}. Depth profiles from under sea ice in the Arctic revealed the highest TEP concentrations, potentially released by sympagic algal activity at the bottom of the sea ice. The aggregation rates in the SML, the interfacial layer between the ocean and atmosphere, were generally enhanced over those in the bulk surface waters by factors of 2 to 30. This finding further strengthens a developing consensus on the gelatinous nature of the SML, which will also affect microbial life, light penetration, and surface wave properties. We present a conceptual model implying that abiotic aggregation is an important factor for TEP production in the ocean, in particular in sea surface microlayers, while consumption by zooplankton and protists recycle TEP, providing a new pool of dissolved precursor material. Overall, TEP is recycled within the water column through heterotrophic grazing and degradation, providing a new pool of TEP precursor materials, while enhanced aggregation rates of TEP in the SML indicates the importance of this thin surface film in the marine carbon cycle.

Citation: Wurl, O., L. Miller, and S. Vagle (2011), Production and fate of transparent exopolymer particles in the ocean, *J. Geophys. Res.*, *116*, C00H13, doi:10.1029/2011JC007342.

1. Introduction

[2] The formation and sinking of biogenic particles mediate vertical mass fluxes, influence optical properties and drive elemental cycling in the ocean, ultimately driving both primary and secondary production and contributing to global climate control. Whereas marine scientists have focused primarily on particle production by phytoplankton growth and aggregation, particle formation by the abiotic assembly of organic macromolecules has been largely neglected.

[3] Transparent exopolymer particles (TEP), ubiquitous and abundant in the ocean, are gels possessing strong surface active properties [*Passow*, 2002]. These particles are mainly formed by abiotic coagulation of dissolved carbohydrates [*Chin et al.*, 1998] excreted by phytoplankton communities. Due to their surface active properties, or "stickiness," TEP act as a glue matrix for other solid particles (i.e., detritus), forming larger aggregates (marine snow) and playing an important role in the export of carbon from the surface to the deep ocean [*Passow et al.*, 2001]. In addition, they represent an essential food source for the benthos and microorganisms residing within the water column below the euphotic zone. Earlier studies have shown that TEP concentrations decrease with depth [*Engel et al.*, 2004], implying at least some consumption by bacteria during sinking.

[4] If unballasted, TEP are positively buoyant and ascend toward the surface to accumulate in the sea surface microlayer (SML), contributing a gelatinous composition to this interfacial film between the ocean and atmosphere [*Wurl and Holmes*, 2008; *Wurl et al.*, 2009]. *Cunliffe and Murrell* [2009] reviewed and discussed the finding of the gelatinous nature of the SML within the context of the bacterioneuston, e.g., bacterial communities residing in the SML. The SML is known to concentrate, to varying degrees, many chemical compounds (i.e., carbohydrates, proteins, and lipids), in particular those that are surface active (surfactants), modifying the chemical and physical properties of the sea surface. For example, the gelatinous, or biofilm-like, composition of the SML may also have significant effects on the penetration of light and UV radiation. For example, *Elasri and Miller* [1999] showed that biofilm matrices adsorb UV radiation to a significant extent. High amounts of surface active substances in the SML also cause wave damping, affecting light reflection and, consequently, penetration.

[1]Institute of Ocean Sciences, Fisheries and Oceans Canada, Sidney, British Columbia, Canada.
[2]Now at Department of Ocean, Earth, and Atmospheric Sciences, Old Dominion University, Norfolk, Virginia, USA.

0148-0227/11/2011JC007342

[5] It has been hypothesized that particle aggregation may be enhanced in the SML due to coagulation of the concentrated dissolved organic matter. *Williams* [1967] wrote: "Detritus derived from the surface films [SML] undoubtedly contributes some fractional part to the particulate organic matter in the euphotic zone and possibly to deep water particulates." Earlier *Riley* [1963] concluded, "Formation on the sea surface seems the only likely explanation for sheet-like aggregates of the order of meter or two in lengths that have been observed occasionally," and although we now know that pelagic invertebrates also contribute to the formation of such aggregates, processes at the sea surface almost certainly contribute, as well. In his seminal paper, *Carlson* [1993] suggested various processes that potentially favor the transformation from dissolved to particulate organic matter, including heterogeneous precipitation, phase changes of surface molecules and repetitive compression and dilation of the sea surface by wave motion. However, to date, none of these speculations have been confirmed.

[6] The aim of this study was to investigate the production and fate of TEP in different regions of the ocean (tropical, temperate and polar). We have investigated the formation rates and accumulation of TEP in the euphotic zone and how these relate to water column stratification, primary production and sea surface conditions. Furthermore, we have investigated TEP production in the SML to test the hypothesis of enhanced particle aggregation in this interfacial boundary layer. The results are tied together with a new conceptual model for the TEP cycle in the ocean.

2. Methods

2.1. Study Areas

[7] Water samples were collected as part of the Radiance in a Dynamic Ocean (RaDyO) project onboard the *R/V Kilo Moana* off Hawaii, on an Arctic research cruise onboard the *CCGS Amundsen* as part of the Canadian ArcticNet program, from the *CCGS J.P. Tully* as part of the Line P and La Perouse programs (see Line P web page provided by Fisheries and Oceans Canada) and from a research ice camp hosted by the Catlin Arctic Survey in the high Canadian Arctic. The ice base was located at N 78° 46.2′ W 104° 43.3′ in Deer Bay, off Ellef Ringnes Island. The water depth at the site of the ice base is unknown but greater than 230 m, as measured with the winch wire. The sampling areas and times represent different trophic states, as well as climatic conditions (Figure 1). Physical and biological features of the sampling areas are presented in Table 1.

2.2. Sample Collection

[8] For this study we collected 16 water column profiles (from the SML down to as deep as 4200 m), plus 12 paired samples from the SML and bulk water at a depth of 1 m. Samples from the SML were collected using a glass plate sampler [*Harvey and Burzell*, 1972] from the bow of a small boat as described in detail by *Wurl et al.* [2011]. The glass plate was immersed vertically and withdrawn gently at a speed of 5–6 cm s^{-1} (as consistently as conditions allowed). Adhering water was removed by wiping the plate with a squeegee into a sample container. The SML thickness collected by this withdrawal rate is about 50 μm [*Carlson*, 1982] and consistent with experimentally determined SML thicknesses of 50 $\pm$ 10 μm using pH microelectrodes [*Zhang et al.*, 2003]. Subsurface samples from 1 m were collected with a 120 mL syringe and weighted polypropylene tubing. Separate subsurface samples from 1 and 8 m were also collected with the syringe and tubing and were filtered onto GF/F filters (47 mm diameter; 500–2000 mL) for chlorophyll-a (Chl-a) analysis. All samples were stored cool during sampling operations. All sampling equipment was washed with 10% HCl and rinsed with ultra pure water prior to use.

[9] Samples from the Catlin ice camp were collected with a Niskin bottle and a hand-operated winch through an ice hole (sea ice thickness about 1.6 m). The ice hole was located about one nautical mile from the camp and about five nautical miles from the nearest shore in water more than 200 m deep. A tent was built over the ice hole to facilitate sampling without freezing and to help keep the hole open between sampling events (typically every 2–3 days), thereby minimizing any disturbances of the underlying water column immediately prior to sampling. Ice slurry from the water surface was removed with a sieve prior to sampling.

[10] At the water column sampling locations (Figure 1), temperature, salinity, fluorescence and dissolved oxygen concentration were measured by CTD casts. In the Pacific, the mixed layer depth (MLD) was estimated as the depth at which temperature differed from the surface by 0.1°C. *Steiner et al.* [2007] showed good agreement between this criterion and MLD derived from modeled turbulent kinetic energy at station P. In the Arctic Ocean (ARC and CAT stations), the MLD was estimated as the depth at which density differed from the surface by 0.125 kg m^{-3}. The depth of the euphotic layer (z_{Eu}) was estimated from the Secchi disk depth (z_{Sec}) as $z_{Eu} = 1.79\ z_{Sec}$ [*Preisendorfer*, 1986].

[11] At the time of SML collection, averaged wind speed was measured using a handheld weather station (Kestrel, Model 3000). We also noted the formation of surface slicks in the sampling area by visual observation. During slick conditions, the concentration of surface active organic materials in the SML exceeds some presently unknown threshold value, and the microlayer becomes visible as smooth gray spots or stripes due to capillary wave damping.

2.3. Chemical Analysis

[12] The TEP concentrations were measured spectrophotometrically according to a dye-binding assay [*Engel*, 2009]. Subsamples (10 to 200 mL) of SML and subsurface water were filtered onto 0.4 μm polycarbonate filters under low vacuum (<100 mm Hg) immediately after collection, stained with 500 μL alcian blue solution (0.02 g alcian blue in 100 mL of acetic acid solution of pH 2.5), and rinsed twice with 1 mL of DI water. Each filter was soaked for 2 h in 6 mL of 80% sulfuric acid (H_2SO_4) to dissolve the dye and then the absorbance of the solution was measured at 787 nm in a 1 cm cuvette. The acidic polysaccharide xanthan gum (Sigma Aldrich) was used as a standard. The detection limit and precision were 4 μg xanthan gum equivalents (Xeq) L^{-1} and better than 13%, respectively. Concentrations in μg Xeq L^{-1} have been converted to carbon (μg C L^{-1}) using the conversion factor of 0.63 [*Engel*, 2004], which is based on a reanalysis of multiple investigations using different phytoplankton cultures and therefore, is appropriate for our study of diverse marine environments.

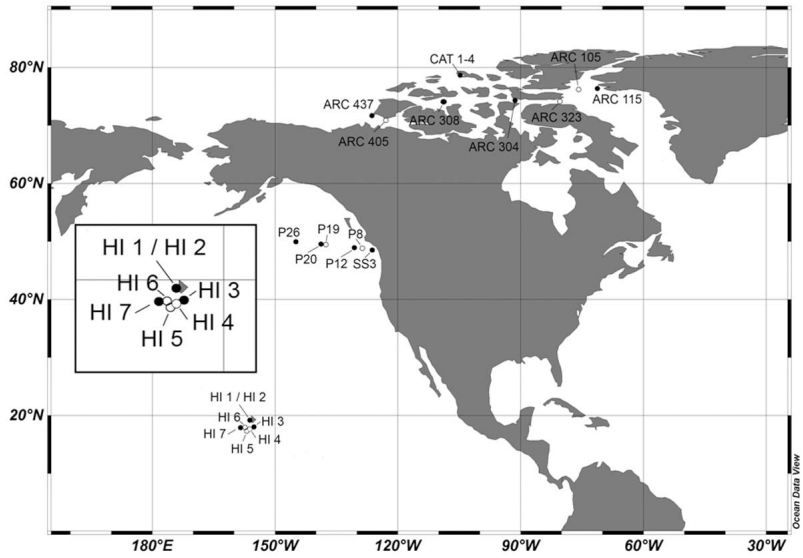

Figure 1. Sampling sites off Vancouver Island (SS), along Line P (P), offshore Hawaii (HI), in the northwest passage (ARC), and at the Catlin ice base (CAT). Black dots represent microlayer and full water column sampling, and white dots represent only microlayer and subsurface water (1 m depth). Note that, for clarity, only the big island of Hawaii is shown.

[13] The concentrations of total dissolved carbohydrates were determined spectrophotometrically using 2,4,6-tripyridyl-s-triazine (TPTZ) as a complexing reagent [*Myklestad et al.*, 1997]. Subsamples for TDC were filtered over 0.2 μm polycarbonate filters prewashed in 10% HCl. Filtrates were stored in precombusted (450°C for 5 h) screw cap test tubes at −20°C for up to 4 weeks. Prior to analysis, the samples were hydrolyzed with 0.85 M H_2SO_4 (final concentration) at 100°C for 24 h to convert polysaccharides to monosaccharides [*Borch and Kirchman*, 1997]. Concentrations of monosaccharides were determined with the same approach in nonhydrolyzed samples, and the concentrations of dissolved polysaccharides (PCHO) were determined by the concentration difference between total carbohydrates and monosaccharides. The procedure typically has a precision better than 7%, based on samples analyzed in triplicate.

[14] Primary production was computed using the Vertical Generalized Production Model (VGPM) [*Behrenfeld and*

Table 1. Physical and Biological Features of Sampling Sites for Water Column Profiles

	Sampling Date	Latitude/ Longitude (deg)	MLD[a] (m)	Chl-a[b] (μg L^{-1}) 1 m	Chl-a[b] (μg L^{-1}) 8 m	PP[b] (g m^{-2} d^{-1}) 1 m	PP[b] (g m^{-2} d^{-1}) 8 m	Depth of Max. FL[c] (m)	Sea Ice Coverage (Visual Observation)
				North Pacific					
SS 3	3 Jun 2009	51.25/−129.35	8.9	1.54	1.72	2.53	n.a.	25.0	
P 12	9 Jun 2009	48.97/−130.67	12.4	0.42	0.43	1.99	0.40	35.6	
P 20	11 Jun 2009	49.57/−138.73	11.0	0.46	0.37	1.65	0.26	37.5	
P 26	14 Jun 2009	50.00/−145.00	12.8	0.30	0.31	1.79	0.26	41.3	
				Offshore Hawaii					
HI 1	27 Aug 2009	19.25/−156.13	21.3	0.53	0.46	0.81	1.04	125.6	
HI 2	28 Aug 2009	19.25/−155.97	22.0	0.63	0.38	1.19	0.86	114.9	
HI 3	1 Sep 2009	17.77/−156.07	39.1	0.52	0.47	0.48	0.44	114.2	
HI 7	9 Sep 2009	18.00/−158.42	31.4	0.42	0.47	0.71	0.66	147.0	
				Arctic Ocean					
ARC 437	14 Oct 2009	71.78/−126.49	29.0	0.34	0.31	0.03	0.03	36.4	0%
ARC 308	19 Oct 2009	74.10/−108.83	13.0	0.14	0.15	0.01	0.01	23.9	100%
ARC 304	23 Oct 2009	74.31/−91.33	26.0	1.68	1.61	0.15	0.14	5.7	100%
ARC 115	29 Oct 2009	76.33/−71.19	20.0	0.71	0.57	0.01	0.01	6.3	0%
CAT 1	25 Mar 2010	78.77/−104.72	12.0	6.40	5.67	n.a.	n.a.	n.a.	100%
CAT 2	18 Apr 2010	78.77/−104.72	12.5	4.20	6.07	n.a.	n.a.	n.a.	100%
CAT 3	22 Apr 2010	78.77/−104.72	14.0	6.90	7.80	n.a.	n.a.	n.a.	100%
CAT 4	24 Apr 2010	78.77/−104.72	13.0	6.57	5.67	n.a.	n.a.	n.a.	100%

[a]Mixed layer depth.
[b]Chlorophyll-a (Chl-a) and primary production (PP) as reported by *Wurl et al.* [2011]. Chl-a data at CAT stations from 3m and 10 m depth.
[c]Maximum fluorescence (FL) reading from conductivity-temperature-depth sensor package.

Table 2. Average Concentrations of TEP (μmol C L^{-1}) and PCHO (μmol C L^{-1}), and dTEP/dt Formation Rates (μmol C L^{-1} d^{-1}) Above and Below the Mixed Layer Depth (MLD) to 250 m

		TEP		PCHO		dTEP/dt	
	Sampling Date	Above MLD	Below MLD	Above MLD	Below MLD	Above MLD	Below MLD
North Pacific							
SS 3	3 Jun 2009	16.0	4.9	10.8	17.8	5.9	4.6
P 12	9 Jun 2009	41.2	14.6	12.8	5.4	14.7	3.4
P 20	11 Jun 2009	8.0	6.4	8.1	14.0	2.8	4.4
P 26	14 Jun 2009	7.0	3.2	17.1	6.8	8.0	0.9
Average ± SD		18.1 ± 15.9	7.3 ± 5.1	12.2 ± 3.8	11.0 ± 5.9	7.9 ± 5.0	3.3 ± 1.7
Offshore Hawaii							
HI 1	27 Aug 2009	37.9	10.9	21.2	23.9	26.8	12.7
HI 2	28 Aug 2009	11.6	8.4	23.2	10.1	10.8	4.8
HI 3	1 Sep 2009	3.9	2.5	25.7	22.0	7.9	5.2
HI 7	9 Sep 2009	3.3	<2.5	10.9	8.9	2.0	1.2
Average ± SD		14.2 ± 16.3	5.8 ± 4.6	20.3 ± 6.5	16.2 ± 7.8	11.9 ± 10.6	6.0 ± 4.8
Arctic Ocean							
ARC 437	12 Oct 2009	11.8	6.1	10.9	19.6	3.8	5.9
ARC 308	19 Oct 2009	5.3	5.0	2.9	6.3	0.6	1.1
ARC 304	23 Oct 2009	6.6	5.2	11.4	11.8	3.0	2.6
ARC 115	29 Oct 2009	18.1	13.4	17.7	16.2	11.8	7.0
Average ± SD		10.5 ± 5.8	7.4 ± 4.0	10.7 ± 6.1	13.5 ± 5.8	4.8 ± 4.9	4.2 ± 2.8
CAT 1	25 Mar 2010	6.5	4.3	11	1.8	3.4	0.3
CAT 2	18 Apr 2010	74.3	43.2	12.0	5.9	23.5	7.6
CAT 3	22 Apr 2010	28.2	16.6	12.1	9.4	12.5	5.0
CAT 4	24 Apr 2010	27.4	17.4	10.8	17.7	9.0	11.9
Average ± SD		33.8 ± 28.7	19.8 ± 16.5	12.2 ± 1.1	8.2 ± 5.8	12.0 ± 8.4	5.6 ± 4.0

Falkowski, 1997] as described by *Wurl et al.* [2011]. For Chl-a determination, filters were extracted into 10 mL of acetone for 24 h at 4°C, with sonication for the first five minutes. Spectrophotometric analysis was conducted according to *Strickland and Parsons* [1972], substituting the equation from *Jeffrey and Humphrey* [1975]. Chlorophyll-a data for the ARC and CAT stations were provided by M. Gosselin (ISMER, Université du Québec à Rimouski) and H. Findlay (Plymouth Marine Laboratory, UK), respectively.

2.4. Validation of Glass Plate Techniques for Collection of TEP

[15] The possibility that TEP from the bulkwater could stick to the glass plate, and thereby appear to be part of the microlayer pool, was of a concern, and we investigated the potential for such a bias. First, we filled acid-washed glass bottles (soda lime glass similar to the glass plate) with seawater of known TEP concentration. After an exposure of ten seconds, equivalent to the time required for a single dip with the glass plate, the water was discharged. Three ml of Alcian blue were added to the bottles to stain the TEP adhering to the walls. Bottles were rotated gently to ensure all surfaces are stained. Staining occurs immediately. Bottles were rinsed with several mL of DI water to remove excessive staining solution. Six ml of 80% sulphuric acid were added to the bottles and extracted for two hours on a rolling table. Control bottles that had not been exposed to seawater were treated similarly. Second, we loaded ten mL of DI water onto horizontal glass plates, which had been used for sampling. After several seconds, the DI water was wiped off with a squeegee directly into a filter funnel for TEP filtration and staining as described in the previous section. This procedure was repeated thrice for each side of the glass plate. Third, the used glass plates from the previous experiment were stained with about ten ml of alcian blue solution, rinsed with DI water, and the stained matter was extracted by carefully rinsing the plate with six mL of 80% sulphuric acid. This experiment did not allow an extraction time of two hours, but shorter extraction time may remove the majority of the stained matter efficiently [*Passow and Alldredge*, 1995].

[16] The amount of TEP extracted from the glass bottle wall was on average 10 ± 4% of the concentration of TEP in the seawater used to fill the bottles. A similar observation was reported by *Ortega-Retuerta et al.* [2009b] and indicates that a small fraction of bulkwater TEP may adhere to the glass plate during sampling. Triplicate experiments on rinsing and wiping (with a squeegee) glass plates that had been exposed to seawater with DI water gave absorbances of 0.161 ± 0.013, 0.199 ± 0.024 and 0.210 ± 0.024 after filtration of the rinses (n = 6 for each experiment) and extraction of TEP-stained filter membranes. The measured absorbances were insignificantly different ($p = 0.2644$, unpaired t test) from the absorbance of pure DI water (abs = 0.209 ± 0.030, n = 4). The results indicate that any TEP stuck to the glass plate is not removed by wiping off adhering water. Final staining of the used glass plates yielded an average absorbance of 0.271 ± 0.077, indicating a small quantity of TEP on the plate, similar to our glass bottle experiments and those of *Ortega-Retuerta et al.* [2009b]. Overall, our results indicate quick adherence of glass surfaces with TEP without any significant effect on the integrity of adhering SML sample. Some TEP from the microlayer may adhere to the plate more persistently too, but based on our bottle experiments, only a small fraction of TEP seems to stick on the glass surface. We also routinely

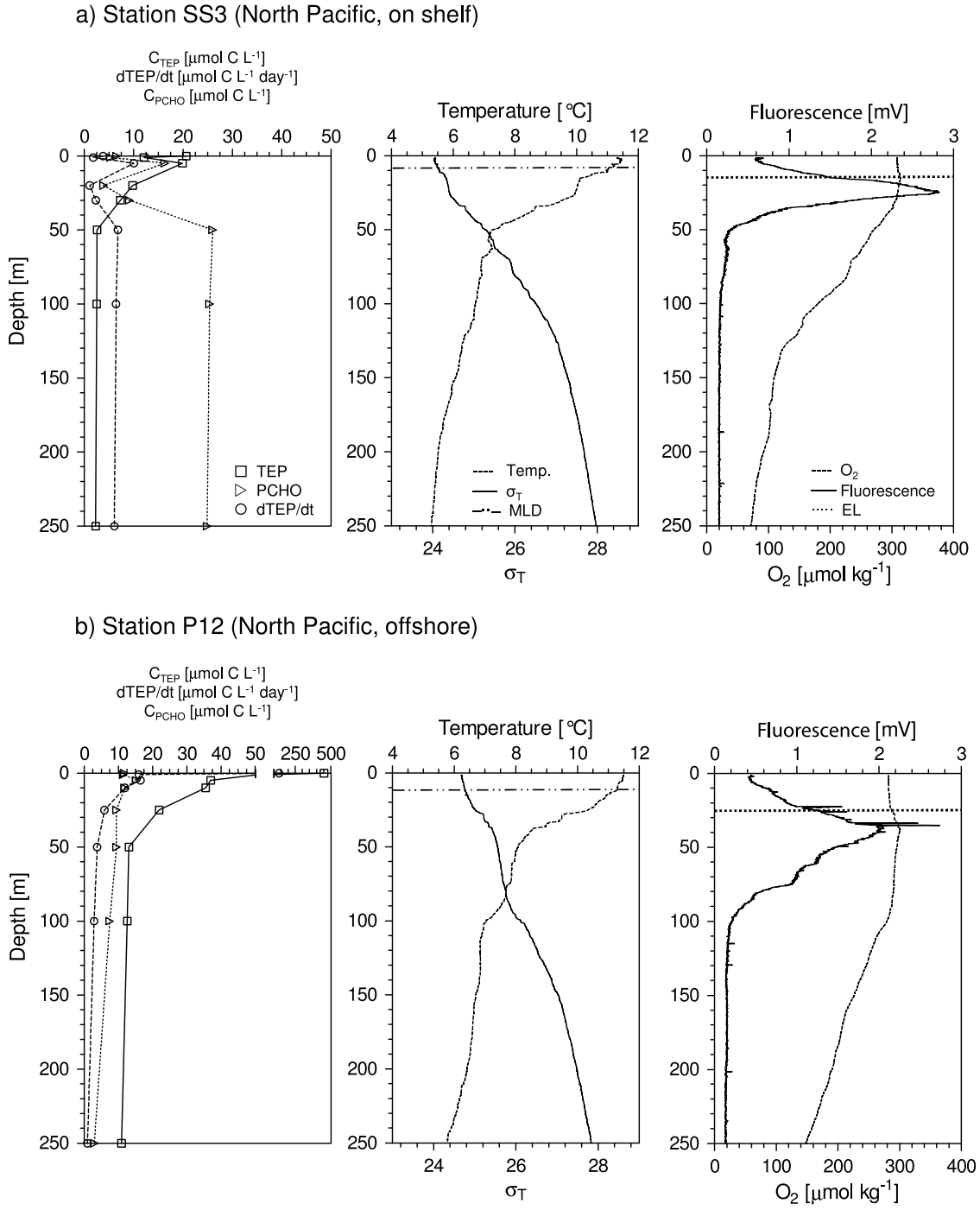

Figure 2. Vertical profiles of TEP (C_{TEP}), dissolved polysaccharides (C_{PCHO}), TEP formation rates (dTEP/dt), temperature, density (σ_T), fluorescence (uncalibrated), and oxygen concentration during cruises in the subpolar North Pacific. Stations (a) SS 3 (on shelf) and (b) P 12 (offshore). MLD, mixed layer depth; EL, euphotic layer depth.

condition the glass plate sampler with 10–15 dips before collecting samples.

2.5. Aggregation Model

[17] Aggregation by physical coagulation requires that primary polymers and particles collide by Brownian motion or advection and then stick together. Coagulation theory as established by *Smoluchowski* [1917] has recently been applied to describe aggregation of marine particles [*Burd and Jackson*, 2009]:

$$\frac{dTEP}{dt} = \alpha_{PCHO}\beta_{PCHO}[PCHO]^2 + \alpha_{TEP}\beta_{TEP}[PCHO][TEP] \quad (1)$$

where [PCHO] is the concentration of dissolved polysaccharide [μmol C L^{-1}], [TEP] is the concentration of TEP

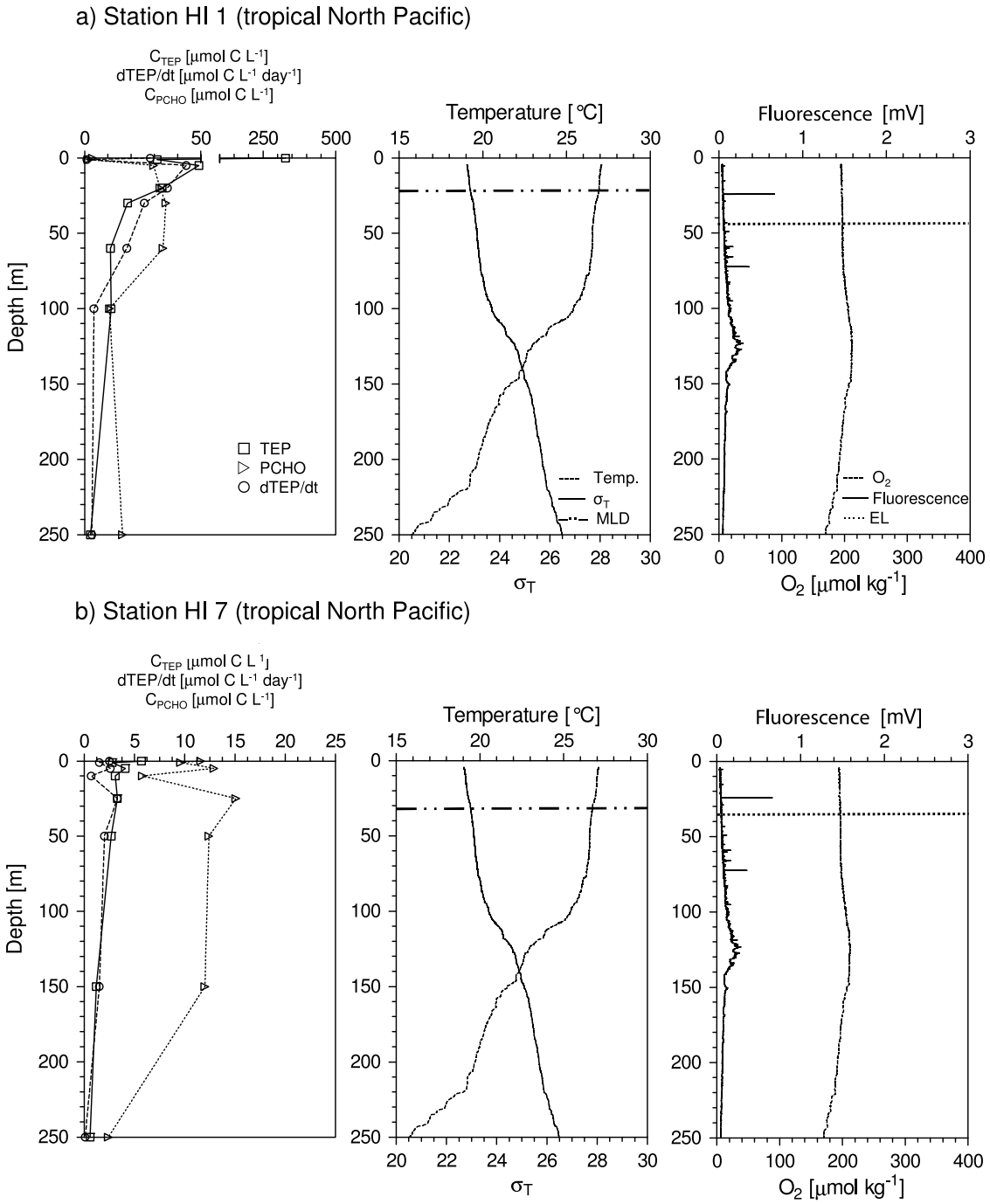

Figure 3. Vertical profiles of TEP (C_{TEP}), dissolved polysaccharides (C_{PCHO}), TEP formation rates (dTEP/dt), temperature, density (σ_T), fluorescence (uncalibrated), and oxygen concentration in the tropical North Pacific, off Hawaii. Stations (a) HI 1 (25 km offshore Hawaii Island) and (b) HI 7 (300 km offshore Hawaii Island). Bottom depth was greater than 1000 m for both stations. MLD, mixed layer depth; EL, depth of euphotic layer.

[μmol C L^{-1}], α_{PCHO} is the self attachment probability of PCHO, α_{TEP} is the attachment probability between PCHO-TEP and β_{PCHO} and β_{TEP} are the carbon-specific collision kernels (collision frequency functions).

[18] *Engel et al.* [2004] showed, during a large-scaled mesocosm study, that such a model is adequate to describe the carbon transfer from dissolved polysaccharides (PCHO) to TEP. *Thoms* [2006] discussed the parameterization of the model in detail.

[19] Here, we use the carbon-specific collision kernel according to *Engel et al.* [2004] as $\beta_{PCHO} = 0.86$ L μmol^{-1} d^{-1} and $\beta_{TEP} = 0.064$ L μmol^{-1} d^{-1}. We also used an attachment probability, α_{PCHO}, of 0.00087, which was determined in mesocosm studies [*Engel et al.*, 2004] and is consistent

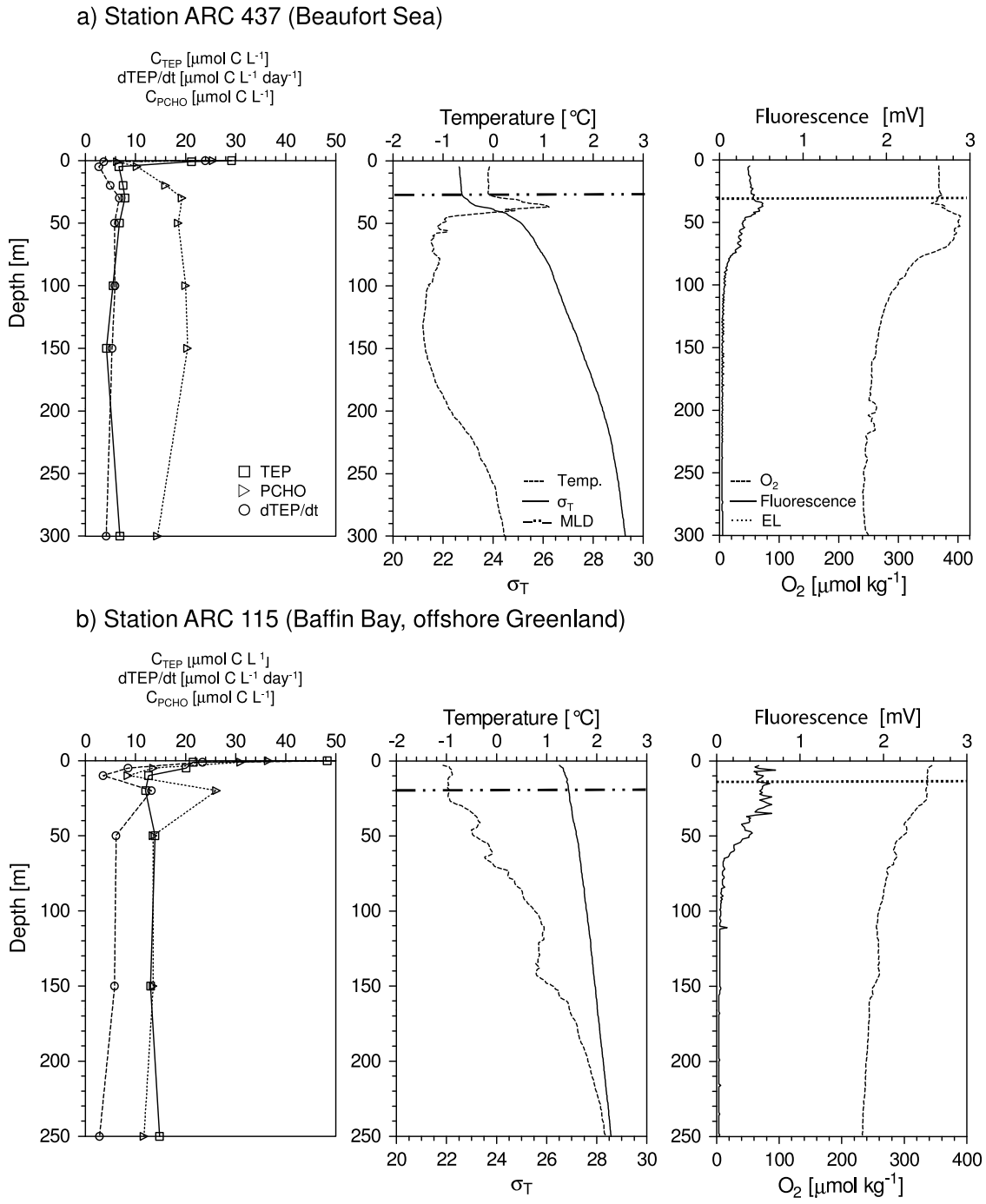

Figure 4. Vertical profiles of TEP (C_{TEP}), dissolved polysaccharides (C_{PCHO}), TEP formation rates (dTEP/dt), temperature, density (σ_T), uncalibrated fluorescence, and oxygen concentration in the southern Canadian Archipelago. Stations (a) ARC 437 and (b) ARC 115. MLD, mixed layer depth; EL, depth of euphotic layer.

with previous estimates of $\alpha_{PCHO} < 0.001$ [*Wells and Goldberg*, 1992]. Attachment probability $\alpha_{PCHO\text{-}TEP}$ can vary between 0.1 and 1 depending on bloom conditions and stage [*Engel*, 2000], and we used the model value of 0.4 from *Engel et al.* [2004]. The attachment probability may vary considerably among the different oceanic regions, and the aggregation rates in Table 2 can only be considered rough estimates. However, we anticipate smaller biases between attachment probabilities at different depths within each station, where the TEP should be derived from the same sources, e.g., the phytoplankton communities.

2.6. Data Analysis

[20] Statistical analyses of the data set were performed using Graphpad PRISM Version 5.1. Differences, null hypothesis testing and correlation were considered to be significant when $p < 0.05$. We tested hypotheses with parametric or nonparametric tests, as stated. The data were log

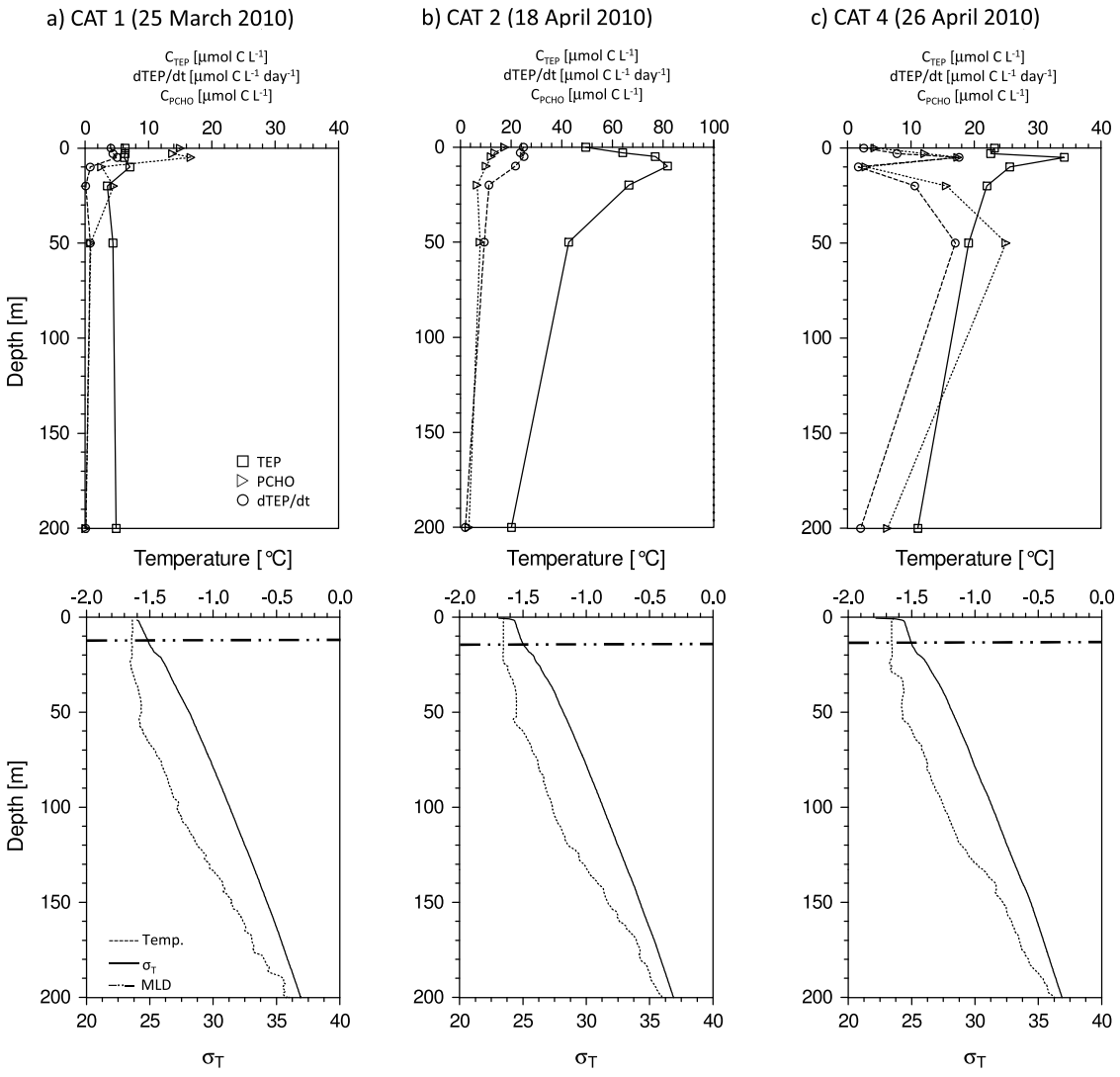

Figure 5. Vertical profiles of TEP (C_{TEP}), dissolved polysaccharides (C_{PCHO}), TEP formation rates (dTEP/dt), temperature, and density (σ_T) in the high Canadian Archipelago, 2010. (a) 25 March 2010, (b) 18 April 2010, and (c) 26 April 2010. MLD, mixed layer depth.

transformed, if required, for parametric and analysis of variance (ANOVA) tests. Unless otherwise indicated, results are presented as means ± standard deviations. Enrichment factors (EF) were calculated as the ratio of concentrations in the SML sample to that of the corresponding subsurface bulk water sample.

3. Results

3.1. Vertical Distribution of TEP in the Water Column

[21] Typical water column profiles of TEP and PCHO concentrations, TEP formation rates and hydrographic parameters are shown in Figures 2–5. The four sample regions (the subpolar North Pacific, the tropical North Pacific, the Northwest Passage, and the high Canadian Archipelago) were characterized by distinctive physical and biological features (Table 1). In the North Pacific (SS and P stations), high fluorescence signals indicate biological activity within the upper 50 m, whereas offshore Hawaii (HI stations) and in the Arctic Ocean (ARC stations), the biological activities were low. At the tropical stations, the maximum productivity occurred at a depth of around 125 m. The mixed layer depth was deepest at the tropical Pacific stations (average 28.3 ± 8.4 m, late summer) and shallowest at the temperate North Pacific stations (average 8.9 ± 1.8 m, early summer).

[22] We did not observe any significant correlation between the Chl-a and TEP concentrations (r = 0.1380, p = 0.2906), contrary to reports in earlier studies [*Passow*, 2002, and references therein; *Wurl and Holmes*, 2008; *Ortega-Retuerta et al.*, 2009a]. However, we also did not observe distinct phytoplankton blooms, resulting in a narrow range of observed Chl-a values (0.30 to 1.58 μg L^{-1}, mean 0.72 ± 0.28 μg L^{-1}), except for CAT stations.

[23] Profiles of TEP concentrations frequently showed higher concentrations above the fluorescence maxima. However, TEP concentrations were consistently higher in the mixed layer than in the deeper waters, while the TEP formation rates were not. Formation rates of TEP were typically

controlled by the concentration of precursor materials (PCHO) (e.g., Figures 2a, 4b, and 5c) through the square of the concentration (see equation (1)). However, at high TEP abundance, the formation rates followed the trend of the TEP concentration (Figures 2b, 3a, 3b, and 5b), and a TEP concentration above 30 μmol L^{-1} appears to be the approximate cutoff between control by TEP versus PCHO.

[24] Overall, the TEP concentrations and formation rates did not vary significantly between the sampling regions (One way ANOVA, p = 0.3387; Table 2), and the fluorescence signal, as an indicator of biological activity, did not correlate with the concentration of TEP in the surface waters. For example, we observed TEP enrichments in the upper water column at stations HI 1 (Figure 3a) and ARC 437 and ARC 115 (Figure 4), despite low biological activity. Occasionally we also observed relatively high TEP formation rates coinciding with low fluorescence signals, i.e., at HI 1 and HI 2 (Table 2) and ARC 115 (Figure 4b).

[25] Residence times of TEP were calculated from TEP concentration divided by formation rate (c_{TEP}/(dTEP/dt)). The overall mean residence time within the mixed layer was 4.6 days (ranging from 0.3 to 34 days). The residence times were essentially the same between the sample locations (One way ANOVA, p = 0.2838). We did observe some longer residence times in the upper water column, but overall, the differences between waters above and below the MLD were insignificant between all sampling regions (Mann-Whitney Test, p > 0.1009).

[26] The profile at station SS 3 (Figure 2a), located on the British Columbian continental shelf (bottom depth 285 m), was distinguished by high concentrations of PCHO below 50 m (up to 26 μmol L^{-1}), controlling TEP formation rates below the mixed layer. In contrast, station P 12 (Figure 2b), located off the shelf (bottom depth 3280 m) was characterized by decreasing PCHO concentrations with depth. Station ARC 437 on the shelf of Banks Island (bottom depth 310 m) was characterized by a pattern of PCHO concentrations similar to that at SS 3 (Figure 4a), indicating that shelf processes may increase the PCHO concentrations below the euphotic layer, thereby also controlling TEP formation. Overall, the PCHO concentrations did not vary significantly between sampling regions, neither in nor below the mixed layer.

[27] Profiles collected under the Arctic sea ice (CAT stations) in early spring were characterized by increases in both TEP and PCHO concentrations with time (Figure 5). The TEP concentration above the MLD increased by more than an order of magnitude over 3 weeks in early April, followed by a loss of more than 50% over the subsequent 8 days (Figure 5). The increase in TEP concentrations and formation rates below the mixed layer observed in the profiles may indicate input from the mixed layer through rapid sinking of TEP aggregates. In contrast, the profiles ARC 304 and 308 (Table 2) collected under the sea ice from an icebreaker (ice broken up by the ship) in the southern Canadian archipelago during autumn were characterized by low TEP concentrations and no significant enrichment in the upper water layers.

[28] Overall, the TEP and PCHO concentrations and the TEP formation rates in deep waters decreased from 250 m toward the bottom in all regions. Concentrations of PCHO were often very low (<2 μmol C L^{-1}) or not detectable below 1000 m. In contrast, we measured low to moderate levels of TEP, between 2 and 7 μmol C L^{-1}, below 2000 m. Resulting TEP formation rates in deep waters were very low (<0.2 μmol C L^{-1} d^{-1}).

3.2. Enrichments of TEP in the Sea Surface Microlayer

[29] Our data show frequent and significant TEP enrichment in the surface microlayer; that is, 89% of the enrichment factors were greater than 1 (Table 3). The mean TEP enrichment was 3.6 $\pm$ 3.4 and was significantly greater than unity (p = 0.0045). The mean enrichments were not significantly different from each other (Kruskal-Wallis test, p = 0.2978) in the different climate zones (Table 3), with the exception of two extreme values observed during a *Trichodesmium* bloom offshore Hawaii. During this bloom, the TEP enrichment, at stations HI 1 and HI 2, was accompanied by extensive slick formation.

[30] In contrast to TEP, the enrichment of PCHO, a precursor material for TEP, was generally lower, ranging between 0.3 and 4.0 with an average value of 1.4 $\pm$ 0.8 (Table 3). 75% of the data indicated enrichments below 1.5, similar to earlier observations [*Wurl et al.*, 2009]. Overall, PCHO enrichment was not significantly different from unity (p = 0.1735).

[31] Despite the low PCHO enrichment, we found that TEP formation rates (dTEP/dt) in the SML were significantly (p = 0.0060, Wilcoxon paired signed rank test) higher, by an average factor of 5, than in waters at 1 m depth (Figure 6). The rates were also significantly more variable in the SML (*F* test, p < 0.0001). Compared to water at a depth of 1 m, and waters from deeper layers, TEP formation rates were typically highest in the SML, and slick conditions seem to favor TEP aggregation (Table 3). The estimated TEP residence times, with respect to formation, averaged 8 days (0.4 to 40 days) in the SML and 6 days (0.3 to 34 days) at 1 m depth, an insignificant difference (Mann-Whitney Test, p = 0.9874).

[32] To evaluate the dynamics of TEP and its precursor material, we compiled a correlation matrix (Table 4). For TEP and PCHO, very significant correlations exist between their concentrations in the SML and in subsurface waters, indicating a dynamic link between those two compartments. The TEP formation rate in the SML ($dTEP/dt_{SML}$) not only correlated significantly with the TEP concentration in the SML, but also with the concentration of TEP in the subsurface water. The enhanced formation rates between the SML and subsurface waters ($dTEP/dt_{Enhanced}$) correlated with both the SML TEP concentration and the PCHO enrichment factor. The negative correlation between wind speed and the TEP concentration in the SML may indicate a process removing TEP from the SML.

4. Discussion

4.1. TEP Accumulation and Dynamics in the Upper Water Column

[33] The objective of this study was to improve our understanding of the production processes and fate of TEP in the upper ocean. To aid this effort, we have used data from this study and from the literature to develop a conceptual model of TEP cycling in the ocean (Figure 7).

[34] Similar to earlier studies [*Engel*, 2004; *Wurl et al.*, 2009], we observed a consistent TEP accumulation within

Table 3. Sampling Conditions and SML Concentrations (CSML and CPCHO, Both in μmol C L^{-1}) and Enrichment Factors (EF) of TEP and PCHO, and TEP Formation Rates in the SML $(dTEP/dt)_{SML}$ (μmol C L^{-1} d^{-1})and Their Enhancement Over Those in Subsurface Waters

	Sampling Date	Latitude/ Longitude (deg)	Wind Speed ($m\ s^{-1}$)	Slick Condition,[a] Y/N	TEP		PCHO		TEP Formation Rates	
					C_{SML}	EF	C_{PCHO}	EF	$(dTEP/dt)_{SML}$	Enhancement
North Pacific										
SS 3	3 Jun 2009	51.25/−129.35	3.8	N	20.7	1.7	6.5	1.2	3.8	2.1
P 8	8 Jun 2009	48.82/−128.67	1.0	marginal	120.4	5.0	2.2	0.7	3.0	0.9
P12	9 Jun 2009	48.97/−130.67	1.6	Y	136.4	8.9	11.7	1.0	136.4	8.6
P 20	11 Jun 2009	49.57/−138.73	1.8	N	18.0	2.5	4.2	n.d.[b]	2.3	n.d.[b]
P 26	14 Jun 2009	50.00/−145.00	6.2	N	18.6	2.6	1.7	1.1	0.9	3.0
P 19	17 Jun 2009	48.50/−137.67	1.9	N	17.7	1.8	18.7	1.2	11.1	1.9
Average ± SD			2.7 ± 1.9		55.3 ± 56.9	3.7 ± 2.8	7.5 ± 6.0	1.1 ± 0.2	26.2 ± 54.1	3.3 ± 3.1
Offshore Hawaii										
HI 1	27 Aug 2009	19.25/−156.13	2.6	Y	327.2	10.5	3.4	2.4	28.3	31.0
HI 2	28 Aug 2009	19.25/−155.97	1.8	Y	161.2	12.1	27.7	1.2	120.1	10.1
HI 3	30 Aug 2009	17.77/−156.07	7.8	N	101.0	2.8	23.7	1.7	65.4	4.6
HI 4	1 Sep 2009	17.77/−156.65	5.2	N	2.9	0.8	27.9	0.9	7.9	0.8
HI 5	5 Sep 2009	17.53/−157.13	6.8	N	19.0	3.6	17.3	2.0	5.7	3.6
HI 6	6 Sep 2009	17.88/−157.42	6.1	N	12.8	1.8	7.3	1.2	2.9	2.9
HI 7	9 Sep 2009	18.00/−158.42	6.2	N	5.7	2.0	11.6	1.2	2.5	1.6
Average ± SD			5.2 ± 2.2		90.0 ± 120.5	4.8 ± 4.5	17.0 ± 9.9	1.5 ± 0.5	33.3 ± 44.4	7.8 ± 10.7
Arctic Ocean										
ARC 437	12 Oct 2009	71.78/−126.49	3.4	N	29.2	1.4	25.5	4.0	23.9	6.5
ARC 405	16 Oct 2009	70.39/−122.59	8.7	N	24.9	2.0	39.4	1.1	36.9	1.8
ARC 323	25 Oct 2009	74.11/−80.82	6.2	N	31.5	1.0	41.9	1.0	47.0	1.0
ARC 105	27 Oct 2009	76.13/−75.53	1.0	N	75.9	2.0	3.8	0.3	7.5	0.6
ARC 115	29 Oct 2009	76.33/−71.19	4.5	N	48.3	2.2	36.5	1.2	55.0	2.4
Average ± SD			4.8 ± 2.9		42.0 ± 21.0	1.7 ± 0.5	29.4 ± 15.6	1.5 ± 1.4	34.1 ± 18.9	2.5 ± 2.4
Overall average ± SD			4.3 ± 2.4		65.1 ± 81.4	3.6 ± 3.4	17.3 ± 13.5	1.4 ± 0.8	31.1 ± 40.7	4.9 ± 7.3

[a]Visual observation of smooth patches around sampling area.
[b]No enrichment due to loss of subsurface sample (n.d., not determined).

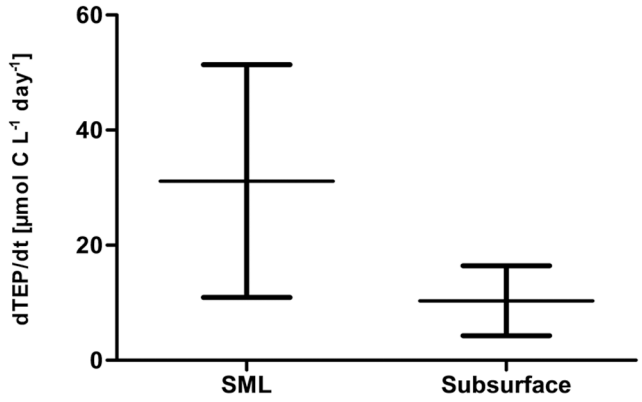

Figure 6. Mean TEP formation rates in the SML and subsurface water (1 m depth) for all paired samples. The bars represent 95% confidence interval of the mean.

the mixed layer (Table 2). A similar consistent accumulation of PCHO, a TEP precursor material, was not evident in the mixed layer, and as a consequence, TEP formation rates were occasionally higher below the MLD. This is because the derived rates are scaled by the square of the PCHO concentration but only by the first order of the TEP concentration (equation (1)). As outlined in section 2.5, the computed aggregation rates are only approximate, due to uncertainties in the TEP attachment probabilities. However, *Mari and Burd* [1998] reported TEP turnover rates (reciprocals of residence times) ranging from 0.1 to 0.9 d^{-1}, which is consistent with the turnover rates computed here. As Mari and Burd used a single steady state particle coagulation model [*Jackson and Lochmann*, 1993] and our approach uses a cluster-cluster model based on Smoluchowski equations, our similar turnover rates derived from the two different models indicate that the chosen attachment probability for TEP of 0.4 is in an environmentally relevant range.

[35] The PCHO concentration typically increases during phytoplankton blooms and especially when phytoplankton become nutrient limited at the end of blooms [*Corzo et al.*, 2000; *Engel et al.*, 2002] ((A) in Figure 7). Polysaccharide exudation by nutrient-starved phytoplankton cells is therefore considered a major pathway in the formation of TEP. Phytoplankton communities in the northern North Pacific (e.g., our P and SS stations) and the Arctic Ocean (our ARC and CAT stations) are typically dominated by diatoms and flagellates [*Boyd and Harrison*, 1999; *Martin et al.*, 2010]. The subtropical waters offshore Hawaii are typically dominated by picoplankton, especially *Synechococcus* [*Boyd et al.*, 2008], although at stations HI 1 and 2, we observed surface blooms of *Trichodesmium* (see section 4.2). Overall, high TEP concentrations have been observed during blooms of diatoms, dinoflagellates and cyanobacteria (i.e., *Trichodesmium*) [*Passow*, 2002], and correlations between chlorophyll-a and TEP concentrations have frequently been observed [*Passow*, 2002, and references therein; *Wurl and Holmes*, 2008; *Ortega-Retuerta et al.*, 2009a]. However, in this study we did not observe a significant correlation between TEP concentration and either the fluorescence signal or chlorophyll-a concentration. Since we did not observe any distinct phytoplankton blooms during our study, our sample set may not be suitable for identifying a correlation between TEP and biomass indicators, due to the narrow and low range of observed chlorophyll values (except CAT stations). We did occasionally observe relatively high TEP formation rates during times of low biological activities (i.e., Figures 3a and 4b), indicative of additional formation and recycling processes, e.g., abotic aggregation of aged dissolved organic matter (DOM) ((C), (E), (P), and (O) in Figure 7).

[36] We suggest that detritus disaggregation can be a source of "aged" DOM and can therefore act as a source for physical DOM to TEP aggregation. *Biddanda and Pomery* [1988] describe the disaggregation process as (1) growth of bacteria, (2) colonization of aggregates by bacteria, (3) detritus aggregation, (4) protozoan growth, (5) consumption of bacteria by protozoans, and (6) disaggregation. Bacteria produce polysaccharide-rich and TEP-like mucus (biological glue) for exploration and attachment to food-rich particles [*Biddanda*, 1986]. In addition, protozoan grazing on bacteria constitute a potential significant source of dissolved surface active material, comparable to estimates of phytoplankton production during blooms [*Kujawinski et al.*, 2002]. Furthermore, zooplankton consume TEP [*Passow and Alldredge*, 1999; *Ling and Alldredge*, 2003] and potentially release surface active substances during feeding [*Croot et al.*, 2007], producing new precursor materials for TEP formation (e.g., recycling: (E), (G) and (O) in Figure 7).

[37] The zooplankton community of the North Pacific (SS and P stations) and the Arctic Ocean (our ARC and CAT stations) are often dominated by calanoid copepods [*Archambault et al.*, 2010]. At the SS and P stations during our cruise, various species of the order Euphausiidae were also found, with more than 10 animals per cubic meter (Line P

Table 4. Correlation Matrix With Pearson Coefficient and p Values (Italicized) on Log-Transformed Data[a]

	Wind Speed	$C_{TEP,SML}$	$C_{TEP,Sub}$	EF_{TEP}	$C_{PCHO,\ SML}$	$C_{PCHO,\ Sub}$	EF_{PCHO}	$dTEP/dt_{SML}$	$dTEP/dt_{Sub}$	$dTEP/dt_{Enhanced}$[b]
Wind speed		**−0.513**	−0.404	−0.440	0.447	0.197	0.425	−0.030	−0.111	0.009
$C_{TEP,SML}$	***0.0294***		**0.846**	**0.789**	−0.171	−0.217	0.002	**0.599**	0.225	**0.551**
$C_{TEP,Sub}$	*0.0965*	***<0.0001***		0.340	−0.007	−0.007	−0.094	**0.627**	0.475	0.240
EF_{TEP}	*0.0677*	***0.0001***	*0.1668*		−0.295	−0.372	0.109	0.334	−0.145	**0.692**
$C_{PCHO,\ SML}$	*0.0631*	*0.4965*	*0.9784*	*0.2351*		**0.864**	0.284	**0.665**	**0.696**	−0.012
$C_{PCHO,\ Sub}$	*0.4479*	*0.4023*	*0.9795*	*0.1410*	***<0.0001***		−0.236	**0.541**	**0.859**	−0.382
EF_{PCHO}	*0.0893*	*0.9950*	*0.7194*	*0.6767*	*0.2686*	*0.3612*		0.206	−0.296	**0.703**
$dTEP/dt_{SML}$	*0.9071*	***0.0086***	***0.0054***	*0.1753*	***0.0026***	***0.0250***	*0.4277*		**0.749**	0.435
$dTEP/dt_{Sub}$	*0.6706*	*0.3850*	*0.0539*	*0.5797*	***0.0019***	***<0.0001***	*0.2481*	***0.0005***		−0.270
$dTEP/dt_{Enhanced}$[a]	*0.9734*	***0.0218***	*0.3541*	***0.0021***	*0.9637*	*0.1307*	***0.0016***	*0.0808*	*0.2942*	

[a]Significant correlation in bold (i.e., $p < 0.05$).
[b]Enhancement factor of TEP formation rates in the SML compared to subsurface water at 1 m depth (Sub).

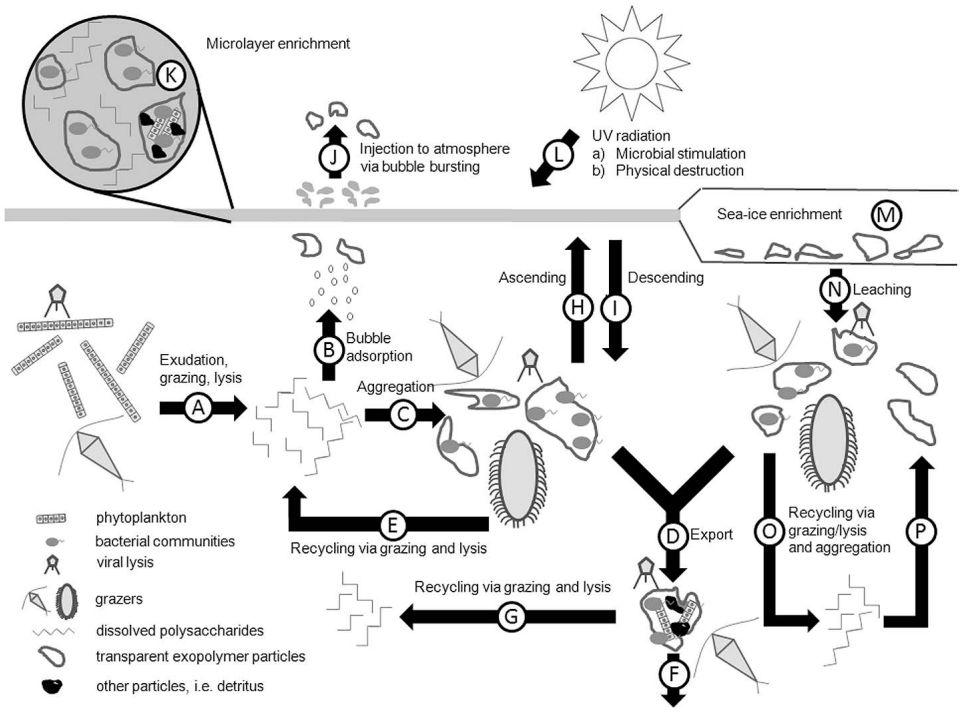

Figure 7. Conceptual model of TEP cycling in the ocean. Capital letters identify processes discussed in the text.

database at www.dfo-mpo.gc.ca). Zooplankton abundances were not investigated at the HI stations, but the literature indicates a dominance of a diverse copepod community in waters at station ALOHA, north of Hawaii [*Hannides et al.*, 2010]. Copepods (*Calanus pacificus*) and Euphausiidae (*Euphausia pacifica)* were used in grazing experiments on TEP by *Passow and Alldredge* [1999] and *Ling and Alldredge* [2003], respectively showing that TEP can be an essential food source even in the presence of phytoplankton cells. Overall, potential grazing on TEP may have occurred during our study.

[38] TEP may also inhibit grazing pressure in later phases of phytoplankton life cycles [*Dutz et al.*, 2005]. The work of Dutz et al. supports the suggestion by *Passow and Alldredge* [1999] that this inhibitory effect is due to TEP ingestion replacing algae as food source for the zooplankton. Furthermore, viral activity produces organic matter through lysis of host cells, thereby releasing organic matter to the dissolved phase [*Middelboe et al.*, 1996; *Gobler et al.*, 1997; *Noble et al.*, 1999]. The released organic matter can also stimulate the growth of new bacterial communities [*Middelboe et al.*, 1996], potentially including colonizing aggregates.

[39] *Biddanda and Pomery* [1988] suggest that detritus aggregation, degradation and disaggregation are continuous processes in the ocean, providing a constant supply of dissolved and aged surface active material for reestablishment of the TEP pool. Assuming that TEP "stickiness" increases with the fraction of aged DOM [*Rochelle-Newall et al.*, 2010], these recycling process can selectively remove the aged TEP pool, as the stickier TEP will aggregate and sink more readily ((D) and (F) in Figure 7). In contrast, the observed accumulation can be explained by fresh, less sticky, TEP remaining in the upper water column. However, fresh TEP may also aggregate in the presence of abundant phytoplankton and sink, particularly toward the end of a bloom [*Thornton*, 2002].

[40] The significant correlations of TEP concentrations in the euphotic zone with TEP formation rates and concentrations in the SML (Table 4) indicate a dynamic link between TEP pools in the surface waters and the SML. Freshly generated TEP, with an average size of 3–4 μm, has a density in the range of 0.7 to 0.8 g cm^{-3} [*Azetsu-Scott and Passow*, 2004] and therefore has the potential to ascend in the water column ((H) in Figure 7). In a water column with a small density gradients (i.e., $\Delta\sigma$ = 1.2 g cm^{-3}), neutral or even positive aggregate buoyancy can be achieved by replacing only 2% of the aggregate interstitial volume with mucus-like substances [*Alldredge and Crocker*, 1995]. While TEP may originate in the euphotic zone, it can grow within the SML through further aggregation, then sink back into the water column ((I) in Figure 7) or be injected into the atmosphere via air bubble bursting ((J) in Figure 7) (see section 4.2).

4.2. TEP Accumulation and Dynamics in the Sea Surface Microlayer

[41] As discussed in section 4.1, we suggest that positively buoyant TEP may rise from the bulk euphotic zone toward the SML. The ascending versus sinking velocities of TEP ((H) and (I) in Figure 7) are controlled by the relative proportions of TEP, POC, and interstitial water within aggregates and by the density of the surrounding water and are therefore, difficult to predict. However, typical POC enrichments in the SML range from 2 to 38 [*Carlson*, 1993], indicating potential interaction between TEP and POC to form heavier aggregates that are prone to sink into the water

column. The fate and turnover rates of TEP in the SML depend on many factors, including POC concentration, bubble bursting, UV radiation and microbial activities, as discussed below.

[42] Perhaps our most fundamental observation is the significantly higher TEP formation rates in the SML compared to subsurface waters (1 m depth) (Figure 6) and the water column below (Table 3). *Riley* [1963] and *Williams* [1967] hypothesized that surface films (e.g., the SML) play an important role in the formation of aggregates (e.g., marine snow). The high TEP formation rates we observed also support the idea that the SML is gelatinous, as first postulated by *Sieburth* [1983] and later confirmed through field experiments [*Wurl and Holmes*, 2008; *Wurl et al.*, 2009; *Cunliffe et al.*, 2009]. The observed TEP accumulation in the upper water column (see section 4.1) and its potential upward flux (high TEP fractions in the particulate organic carbon (POC)) may also constitute an important input of gelatinous material to the SML ((H) in Figure 7). However, in the following, we discuss other processes potentially leading to high TEP formation rates within the SML itself ((K) in Figure 7).

[43] In his review of organic matter transformations in the microlayer, *Carlson* [1993] suggested that constant compression and dilation of the SML can facilitate particle aggregation and condensation of high molecular weight materials. *Wheeler* [1975] experimentally compressed the SML of Nova Scotian lakes and coastal waters to investigate the transformation of dissolved (DOM) into particulate organic matter (POM). He demonstrated the conversion of DOM to POM through compression of SML on lakes, but productive coastal waters needed to be compressed by 90% of the original area. However, from his report, it is unclear how he confirmed in situ POM formation; he likely used only visual observation. For that reason, he likely was unable to identify any aggregation of smaller sized (10–200 μm) or transparent gel-like particles such as TEP. It is well known that the enrichment of dissolved organic carbon (DOC) in the SML is small, except in surface slicks [*Carlson*, 1983]. However, the enrichment of POC can be very large [*Carlson*, 1993], supporting Wheeler's first observations of organic matter convert between the dissolved and particulate phases in the SML.

[44] As in our earlier study [*Wurl et al.*, 2009], we found a negative correlation between wind speed and TEP concentration in the SML (Table 4), indicating removal processes through deep mixing or bursting bubbles at the surface ((J) in Figure 7). The latter process is supported by the presence of gel-like material in airborne aggregates [*Leck and Bigg*, 2005]. *Russell et al.* [2010] reported the carbohydrate-like composition of aerosols collected over the open ocean and suggested that organic components from the microlayer influence the composition of aerosols produced by bubble bursting, and it can be postulated that the SML contributes to the production of globally relevant aerosols and their properties. However, on one occasion (at HI 3), we found high TEP concentrations and formation rates in the microlayer under relatively high wind speeds (7.8 m s^{-1}, Table 3). We suggest that only under limited conditions (i.e., when the concentrations of TEP precursors like PCHO are high in the subsurface water, (Table 2)) TEP production by bubbles rising through the subsurface water [*Zhou et al.*, 1998] ((B) in Figure 7) can exceed TEP removal from the SML by turbulent processes.

[45] Slick conditions were always found to be associated with high TEP concentrations and formation rates in the microlayer (Table 3). The work of both *Carlson* [1987] and *Van Vleet and Williams* [1983] indicates that molecular rotation is limited in microlayer slicks, possibly leading to different orientations between molecules in the SML than what would occur in bulk water, inducing unique molecular interactions and transformation processes in the microlayer. Such transformation processes include the formation of high-molecular weight molecules (HMW) and polymers, potentially precursor material for TEP.

[46] At stations HI 1 and 2, we observed an intensive *Trichodesmium* bloom with visible colonies floating on the surface. The sea surface was not only smooth and covered by a visible slick in the region of the bloom but also was characterized by high TEP concentrations and formation rates (Table 3). Slicks associated *Trichodesmium* blooms have also been observed by *Sieburth and Conover* [1965], who explained the slicks by carbohydrate excretion by *Trichodesmium*. *Young* [1977] observed that SML bacterial communities are also able to excrete considerable amounts of polymeric materials. Such extracellular polymers potentially aggregate into TEP. Laboratory experiments suggest that bacterial communities in the SML excrete these polymeric materials as protection against strong UV radiation ((L) in Figure 7) [*Elasri and Miller*, 1999; *Ortega-Retuerta et al.*, 2009b]. Such a protective mechanism could therefore significantly contribute to the gelatinous nature of the SML. In the absence of microorganisms, *Ortega-Retuerta et al.* [2009b] reported losses of TEP exposed to UV-B via photolysis ((L) in Figure 7). Overall, our results indicate that high TEP formation rates in the SML facilitate the production of a gel-like habitat for microorganisms [*Cunliffe et al.*, 2011]. Therefore, we suggest that the SML has a unique role in the marine microbial loop and the carbon cycle.

4.3. TEP Accumulation and Dynamics Under Arctic Sea Ice

[47] Under the sea ice during the transition from winter to spring, we observed some of the highest water column TEP concentrations and formation rates of our entire study (Table 2 and Figure 5b). Abundances of diatoms were low in the water column but increased during our study from 0.4 cell ml^{-1} (25 March 2010) to 2.9 cells ml^{-1}. Nanoplankton dominated the community, with counts ranging between 28,000 and 136,000 cells ml^{-1} (H. Findlay, personal communication, 2011). A number of studies have reported high concentrations of exopolymeric substances in sea ice ((M) in Figure 7) [*Krembs et al.*, 2002; *Meiners et al.*, 2003; *Riedel et al.*, 2006; *Collins et al.*, 2008], and we suggest that the large EPS pulse we observed at the Catlin camp was the result of discharge from the ice with draining brines.

[48] *Krembs et al.* [2002] reported the first TEP time series from sea ice and found that the concentration in land fast ice increased throughout the winter. They suggested that TEP may act as a cryoprotectant for diatoms trapped in freezing sea ice. Thus, high TEP concentrations would not be expected in new autumn sea ice or its underlying waters, consistent with our October observations in the southern Canadian Achipelago. *Riedel et al.* [2006] and *Collins et al.*

[2008] both also studied seasonal trends of exopolymeric substances (EPS, analytically equivalent to our TEP) in land fast sea ice, and they confirmed that EPS increased in the ice with time, with concentrations beginning to rise earlier in the season higher up in the ice column, closer to the ice-air interface. *Riedel et al.* [2006] suggested that light availability to the algal communities in the sea ice limited their ability to excrete TEP. However, evidence from a number of studies has indicated that the bacterial community is also likely to affect carbon cycling and EPS concentration and distribution within sea ice [*Junge et al.*, 2004; *Collins et al.*, 2008; *Deming*, 2010; *Krembs et al.*, 2011; *Miller et al.*, 2011].

[49] *Riedel et al.* [2006] measured very low EPS concentrations in surface waters at the ice-water interface (up to 3.7 μmol C L^{-1}, based on a carbon conversion factor of 0.63), similar to the concentrations we observed in under ice waters on 25 March (CAT 1). However, contrary to our observations, Riedel et al. did not observe a large surface water EPS increase, despite their approximately 5 day sampling resolution from early March to late May. The short life span of the TEP pulse we observed, with a substantial decline after only 8 days, implies rapid removal and/or recycling, and Riedel et al. sampled only at the ice-water interface. During their study, the surface water was highly stratified by a low-salinity lens beneath the ice (B. Lansard et al., Seasonal variability of water mass distribution in the southeastern Beaufort Sea determined by total alkalinity and $\delta^{18}O$, submitted to *Journal of Geophysical Research*, 2011), and therefore, they could have missed a rapid pulse of EPS released from the ice, if it quickly sank away from the ice-water interface and mixed into the polar mixed layer at 10–20 m. Another possible explanation for the discrepancy between the water column EPS dynamics in our study and that of *Riedel et al.* [2006] is that high EPS concentrations within the ice can reduce brine drainage and ice melt rates [*Krembs et al.*, 2011], which would in turn limit EPS release from the ice. We did not measure EPS concentrations in the sea ice at our sampling site, but *Riedel et al.* [2006] found very high concentrations comparable to those observed by *Krembs et al.* [2011]. Therefore, EPS release to the underlying water may have also been inhibited at the site studied by *Riedel et al.* [2006]. The increase in TEP concentrations in the surface waters between 25 March and 18 April (Figures 5a and 5b) is remarkable, but so are the rapid losses during the following 8 days (Figure 5c). The parallel increase in TEP formation rates below the mixed layer between 18 and 24 April suggests that much of the TEP lost from the surface sank into deeper waters.

5. Conclusion

[50] During this study we found surprisingly high TEP concentrations in waters with low primary production, indicating that abiotic aggregation of dissolved organic matter can be a source of TEP in the absence of phytoplankton blooms. Apparently, TEP is recycled within the water column through heterotrophic grazing and degradation, providing input of TEP precursor materials. Nonetheless, primary production is the ultimate source of precursor materials in all cases.

[51] The highest concentrations of TEP in the mixed layer were found under early spring Arctic sea ice. Brine drainage from warming ice and the onset of photosynthetic activity in the bottom ice community are the likely sources of the observed high TEP concentrations. However, rapid TEP losses can occur, presumably due to sinking and grazing.

[52] Formation rates of TEP are significantly higher in the SML compared to underlying waters. Constant compression and dilation through wave action may enhance the collision between organic compounds and facilitate TEP formation and growth. High exposure to UV light may also trigger bacterial TEP production in the SML as a protective shield against harmful radiation. At high wind states, TEP in the SML is likely lost to the atmosphere through bubble bursting and to the underlying water column by deep mixing.

[53] With our new findings and the existing literature, we have developed a conceptual model for the production and fate of TEP in surface waters. This model can help target future research priorities to improve our understanding of TEP cycling, including carbon sequestration to the deep ocean, TEP as food source for plankton and the role of TEP in the formation of organic-rich aerosols affecting formation of cloud condensation nuclei.

[54] **Acknowledgments.** The authors would like to thank Fisheries and Oceans Canada, the Office of Naval Research (ONR, Contract N 000140710754) and ArcticNet for financial support. This study also draws on data obtained as part of the Catlin Arctic Survey whose resources were made possible by the funding support of the Catlin Group. O. Wurl thanks the Deutsche Forschungsgemeinschaft (DFG) for a postdoctoral scholarship (WU 585/2–1). We thank Keith Johnson, Glenn Cooper, Eunice Wurl, the officers and crews of CCGS *JP Tully*, RV *Kilo Moana*, and CCGS *Amundsen*, the team of the Catlin Ice Base, and Geo Mission Ltd. for their invaluable support during sample collection and processing. We thank M. Gosselin and H. Findlay for chlorophyll data for ARC and CAT stations, respectively.

References

Alldredge, A. L., and K. M. Crocker (1995), Why do sinking mucilage aggregates accumulate in the water column?, *Sci. Total Environ.*, *165*, 15–22, doi:10.1016/0048-9697(95)04539-D.

Archambault, P., et al. (2010), From sea to sea: Canada's three oceans of biodiversity, *PLoS One*, *5*(8), e12182, doi:10.1371/journal.pone.0012182.

Azetsu-Scott, K., and U. Passow (2004), Ascending marine particles: Significance of transparent exopolymer particles (TEP) in the upper ocean, *Limnol. Oceanogr.*, *49*(3), 741–748, doi:10.4319/lo.2004.49.3.0741.

Behrenfeld, M. J., and P. G. Falkowski (1997), A consumer's guide to phytoplankton primary productivity models, *Limnol. Oceanogr.*, *42*(7), 1479–1491, doi:10.4319/lo.1997.42.7.1479.

Biddanda, B. A. (1986), Structure and function of marine microbial aggregates, *Oceanol. Acta*, *9*, 209–211.

Biddanda, B. A., and L. R. Pomery (1988), Microbial aggregation and degradation of phytoplankton-derived detritus in seawater. I. Microbial succession, *Mar. Ecol. Prog. Ser.*, *42*, 79–88, doi:10.3354/meps042079.

Borch, N. H., and D. L. Kirchman (1997), Concentration and composition of dissolved combined neutral sugars (polysaccharides) in seawater determined by HPLC-PAD, *Mar. Chem.*, *57*, 85–95, doi:10.1016/S0304-4203(97)00002-9.

Boyd, P., and P. J. Harrison (1999), Phytoplankton dynamics in the NE subarctic Pacific, *Deep Sea Res., Part II*, *46*, 2405–2432, doi:10.1016/S0967-0645(99)00069-7.

Boyd, P. W., M. P. Gall, M. W. Silver, S. L. Coale, R. R. Bidigare, and J. L. K. B. Bishop (2008), Quantifying the surface–subsurface biogeochemical coupling during the VERTIGO ALOHA and K2 studies, *Deep Sea Res., Part II*, *55*, 1578–1593, doi:0.1016/j.dsr2.2008.04.010.

Burd, A. B., and G. A. Jackson (2009), Particle aggrenation, *Annu. Rev. Mar. Sci.*, *1*, 65–90, doi:10.1146/annurev.marine.010908.163904.

Carlson, D. J. (1982), A field evaluation of plate and screen microlayer sampling techniques, *Mar. Chem.*, *11*, 189–208, doi:10.1016/0304-4203(82)90015-9.

Carlson, D. J. (1983), Dissolved organic materials in surface microlayers: Temporal and spatial variability and relation to sea state, *Limnol. Oceanogr.*, *28*, 415–431, doi:10.4319/lo.1983.28.3.0415.

Carlson, D. J. (1987), Viscosity of sea-surface slicks, *Nature*, *329*, 823–825, doi:10.1038/329823a0.

Carlson, D. J. (1993), The early diagenesis of organic matter: Reaction at the air–sea interface, in *Organic Geochemistry*, edited by M. H. Engel and S. A. Macko, pp. 255–268, Plenum Press, New York, doi:10.1007/978-1-4615-2890-6_12.

Chin, W.-C., M. V. Orellana, and P. Verdugo (1998), Spontaneous assembly of marine dissolved organic matter in polymer gels, *Nature*, *391*, 568–572, doi:10.1038/35345.

Collins, R. E., S. D. Crapenter, and J. W. Deming (2008), Spatial heterogeneity and temporal dynamics of particles, bacteria, and pEPS in Arctic winter sea ice, *J. Mar. Syst.*, *74*, 902–917, doi:10.1016/j.jmarsys.2007.09.005.

Corzo, A., J. A. Morillo, and S. Rodríguez (2000), Production of transparent exopolymer particles (TEP) in cultures of *Chaetoceros calcitrans* under nitrogen limitation, *Aquat. Microb. Ecol.*, *23*(1), 63–72, doi:10.3354/ame023063.

Croot, P. L., U. Passow, P. Assmy, S. Jansen, and V. H. Strass (2007), Surface active substances in the upper water column during a Southern Ocean Iron Fertilization Experiment (EIFEX), *Geophys. Res. Lett.*, *34*, L03612, doi:10.1029/2006GL028080.

Cunliffe, M., and J. C. Murrell (2009), The sea-surface microlayer is a gelatinous biofilm, *ISME J.*, *3*, 1001–1003, doi:10.1038/ismej.2009.69.

Cunliffe, M., M. Salter, P. J. Mann, A. S. Whiteley, R. C. Upstill-Goddard, and J. C. Murrell (2009), Dissolved organic carbon and bacterial populations in the gelatinous surface microlayer of a Norwegian fjord mesocosm, *FEMS Microbiol. Lett.*, *299*(2), 248–254, doi:10.1111/j.1574-6968.2009.01751.x.

Cunliffe, M., R. C. Upstill-Goddard, and J. C. Murrell (2011), Microbiology of aquatic surface microlayers, *FEMS Microbiol. Rev.*, *35*(2), 233–246, doi:10.1111/j.1574-6976.2010.00246.x.

Deming, J. W. (2010), Sea ice bacteria and viruses, in *Sea ice*, 2nd ed., edited by D. N. Thomas and G. S. Dieckmann, pp. 247–282, Wiley-Blackwell, Oxford, U. K.

Dutz, J., W. C. M. Klein Breteler, and G. Kramer (2005), Inhibition of copepod feeding by exudates and transparent exopolymer particles (TEP) derived from a *Phaeocystis globosa* dominated phytoplankton community, *Harmful Algae*, *4*, 929–940.

Elasri, M. O., and R. V. Miller (1999), Study of the response of a biofilm bacterial community to UV radiation, *Appl. Environ. Microbiol.*, *65*, 2025–2031.

Engel, A. (2000), The role of transparent exopolymer particles (TEP) in the increase in apparent particle stickiness (α) during the decline of a diatom bloom, *J. Plankton Res.*, *22*, 485–497, doi:10.1093/plankt/22.3.485.

Engel, A. (2004), Distribution of transparent exopolymer particles (TEP) in the northeast Atlantic Ocean and their potential significance for aggregation processes, *Deep Sea Res., Part I*, *51*, 83–92, doi:10.1016/j.dsr.2003.09.001.

Engel, A. (2009), Determination of marine gel particles, in *Practical Guidelines for the Analysis of Seawater*, edited by O. Wurl, pp. 125–142, CRC Press, Boca Raton, Fla., doi:10.1201/9781420073072.ch7.

Engel, A., S. Goldthwait, U. Passow, and A. Alldredge (2002), Temporal decoupling of carbon and nitrogen dynamics in a mesocosm diatom bloom, *Limnol. Oceanogr.*, *47*(3), 753–761, doi:10.4319/lo.2002.47.3.0753.

Engel, A., S. Thoms, U. Riebesell, E. Rochelle-Newall, and I. Zondervan (2004), Polysaccharide aggregation as a potential sink of marine dissolved organic carbon, *Nature*, *428*, 929–932, doi:10.1038/nature02453.

Gobler, C. J., D. A. Hutchins, N. S. Fisher, E. M. Cosper, and S. Sañudo-Wilhelmy (1997), Release and bioavailability of C, N, P, Se, and Fe following viral lysis of a marine chrysophyte, *Limnol. Oceanogr.*, *42*(7), 1492–1504, doi:10.4319/lo.1997.42.7.1492.

Hannides, C., M. Landry, and B. Popp (2010), Understanding climate-driven change in zooplankton communities: A case study from the North Pacific Subtropical Gyre, in *Proceedings of the Joint ICES/CIESM Workshop to Compare Zooplankton Ecology and Methodologies between Mediterranean and the North Atlantic (WKZEM)*, edited by A. Gislason and G. Gorsky, *Coop. Res. Rep. 300*, pp. 35–39, Int. Counc. for the Explor. of the Sea, Copenhagen.

Harvey, G. W., and L. A. Burzell (1972), A simple microlayer method for small samples, *Limnol. Oceanogr.*, *17*(1), 156–157, doi:10.4319/lo.1972.17.1.0156.

Jackson, G. A., and S. E. Lochmann (1993), Modelling coagulation of algae in marine ecosystems, in *Environmental particles*, *Environ. Anal. and Phys. Chem. Ser.*, vol. 2, edited by J. Buffle and H. P. van Leeuwen, pp. 387–414, Lewis Publ., Boca Raton, Fla.

Jeffrey, S. W., and G. F. Humphrey (1975), New spectrophotometric equations for determining chlorophylls a, b, c1 and c2 in higher plants, algae and natural phytoplankton, *Biochem. Physiol. Pflanz.*, *167*, 191–194.

Junge, K., H. Eicken, and J. W. Deming (2004), Bacterial activity at −2 to −20°C in Arctic wintertime sea ice, *Appl. Environ. Microbiol.*, *70*(1), 550–557, doi:10.1128/AEM.70.1.550-557.2004.

Krembs, C., H. Eicken, K. Junge, and J. W. Deming (2002), High concentrations of exopolymeric substances in Arctic winter sea ice: Implications for the polar ocean carbon cycle and cryoprotection of diatoms, *Deep Sea Res., Part I*, *49*, 2163–2181, doi:10.1016/S0967-0637(02)00122-X.

Krembs, C., H. Eicken, and J. W. Deming (2011), Exopolymer alteration of physical properties of sea ice and implications for ice habitability and biogeochemistry in a warmer Arctic, *Proc. Natl. Acad. Sci. U. S. A.*, *108*(9), 3653–3658, doi:10.1073/pnas.1100701108.

Kujawinski, E. B., J. F. Farrington, and J. W. Moffet (2002), Evidence for grazing-mediated production of dissolved surface-active material by marine protists, *Mar. Chem.*, *77*(2–3), 133–142, doi:10.1016/S0304-4203(01)00082-2.

Leck, C., and E. K. Bigg (2005), Biogenic particles in the surface microlayer and overlaying atmosphere in the central Arctic Ocean during summer, *Tellus, Ser. B*, *57*, 305–316.

Ling, S. C., and A. L. Alldredge (2003), Does the marine copepod *Calanus pacificus* consume transparent exopolymer particles (TEP)?, *J. Plankton Res.*, *25*(5), 507–515, doi:10.1093/plankt/25.5.507.

Mari, X., and A. Burd (1998), Seasonal size spectra of transparent exopolymeric particles (TEP) in a coastal sea and comparison with those predicted using coagulation theory, *Mar. Ecol. Prog. Ser.*, *163*, 63–76, doi:10.3354/meps163063.

Martin, J., J. E. Tremblay, J. Gagnon, G. Tremblay, A. Lapoussière, C. Jose, M. Poulin, M. Gosselin, Y. Gratton, and C. Michel (2010), Prevalence, structure, and properties of subsurface chlorophyll maxima in Canadian Arctic waters, *Mar. Ecol. Prog. Ser.*, *412*, 69–84, doi:10.3354/meps08666.

Meiners, K., R. Gradinger, J. Fehling, G. Civitarese, and M. Spindler (2003), Vertical distribution of exopolymer particles in sea ice of the Fram Strait (Arctic) during autumn, *Mar. Ecol. Prog. Ser.*, *248*, 1–13, doi:10.3354/meps248001.

Middelboe, M., N. O. G. Jørgensen, and N. Kroer (1996), Effects of viruses on nutrient turnover and growth efficiency of noninfected marine bacterioplankton, *Appl. Environ. Microbiol.*, *62*, 1991–1997.

Miller, L. A., T. N. Papkyriakou, R. E. Collins, J. W. Deming, J. K. Ehn, R. W. Macdonald, A. Mucci, O. Owens, M. Raudsepp, and N. Sutherland (2011), Carbon dynamics in sea ice: A winter flux time series, *J. Geophys. Res.*, *116*, C02028, doi:10.1029/2009JC006058.

Myklestad, S. M., E. Skånøy, and S. Hestman (1997), A sensitive and rapid method for analysis of dissolved mono- and polysaccharides in seawater, *Mar. Chem.*, *56*, 279–286, doi:10.1016/S0304-4203(96)00074-6.

Noble, R. T., M. Middelboe, and J. A. Fuhrman (1999), The effects of viral enrichment on the mortality and growth of heterotrophic bacterioplankton, *Aquat. Microb. Ecol.*, *18*, 1–13.

Ortega-Retuerta, E., I. Reche, E. Pulido-Villena, S. Agustí, and C. M. Duarte (2009a), Uncoupled distributions of transparent exopolymer particles (TEP) and dissolved carbohydrates in the Southern Ocean, *Mar. Chem.*, *115*, 59–65.

Ortega-Retuerta, E., U. Passow, C. M. Duarte, and I. Reche (2009b), Effects of ultraviolet B radiation on (not so) transparent exopolymer particles, *Biogeosciences*, *6*, 3071–3080, doi:10.5194/bg-6-3071-2009.

Passow, U. (2002), Transparent exopolymer particles (TEP) in aquatic environments, *Prog. Oceanogr.*, *55*, 287–333, doi:10.1016/S0079-6611(02)00138-6.

Passow, U., and A. L. Alldredge (1995), A dye-binding assay for the spectrophotometric measurement of transparent exopolymer particles (TEP), *Limnol. Oceanogr.*, *40*(7), 1326–1335.

Passow, U., and A. L. Alldredge (1999), Do transparent exopolymer particles (TEP) inhibit grazing by the euphausiid *Euphausia pacifica*?, *J. Plankton Res.*, *21*(11), 2203–2217, doi:10.1093/plankt/21.11.2203.

Passow, U., R. F. Shipe, A. Murray, D. K. Pak, M. A. Brzezinski, and A. L. Alldredge (2001), The origin of transparent exopolymer particles (TEP) and their role in the sedimentation of particulate matter, *Cont. Shelf Res.*, *21*, 327–346, doi:10.1016/S0278-4343(00)00101-1.

Preisendorfer, R. W. (1986), Secchi disk science: Visual optics of natural waters, *Limnol. Oceanogr.*, *31*(5), 909–926, doi:10.4319/lo.1986.31.5.0909.

Riedel, A., C. Michel, and M. Gosselin (2006), Seasonal study of sea-ice exopolymeric substances on the Mackenzie shelf: Implications for transport of sea-ice bacteria and algae, *Aquat. Microb. Ecol.*, *45*, 195–206, doi:10.3354/ame045195.

Riley, G. A. (1963), Organic aggregates in seawater and the dynamics of their formation and utilization, *Limnol. Oceanogr.*, *8*(4), 372–381, doi:10.4319/lo.1963.8.4.0372.

Rochelle-Newall, E. J., X. Mari, and O. Pringault (2010), Sticking properties of transparent exopolymeric particles (TEP) during aging and biodegradation, *J. Plankton Res.*, *32*(10), 1433–1442, doi:10.1093/plankt/fbq060.

Russel, L. M., L. N. Hawkins, A. A. Frossard, P. K. Quinn, and T. S. Bates (2010), Carbohydrate-like composition of submicron atmospheric particles and their production from ocean bubble bursting, *Proc. Natl. Acad. Sci. U. S. A.*, *107*, 6652–6657.

Sieburth, J. (1983), Microbiological and organic-chemical processes in the surface and mixed layers, in *Air-Sea Exchange of Gases and Particles*, edited by P. S. Liss and W. G. N. Slinn, pp. 121–172, D. Reidel, Hingham, Mass.

Sieburth, J., and J. T. Conover (1965), Slicks associated with *Trichodesmium* blooms in the Saragossa Sea, *Nature*, *205*, 830–831, doi:10.1038/205830b0.

Smoluchowski, M. (1917), Versuch einer mathematischen Theorie der Koagulationskinetic kolloider Lösungen, *Z. Phys. Chem.*, *92*, 129–168.

Steiner, N., S. Vagle, K. Denman, and C. McNeil (2007), Oxygen and nitrogen cycling in the northeast Pacific: Simulations and observations at Station Papa in 2003/2004, *J. Mar. Res.*, *65*(3), 441–469.

Strickland, J. D., and T. R. Parsons (1972), *A Practical Handbook of Seawater Analysis*, Fisheries Res. Board of Canada, Ottawa.

Thoms, S. (2006), Parameterization of coagulation processes in the formation of transparent exopolymer particles (TEP), paper presented at International Workshop on Marine Aggregates (IWOMA), Max Planck Inst. for Mar. Microbiol., Bremen, Germany, 11–12 Dec.

Thornton, D. (2002), Diatom aggregation in the sea: Mechanisms and ecological implications, *Eur. J. Phycol.*, *37*, 149–161, doi:10.1017/S0967026202003657.

Van Vleet, E. S., and P. M. Williams (1983), Surface potential and film pressure measurements in seawater systems, *Limnol. Oceanogr.*, *28*(3), 401–414, doi:10.4319/lo.1983.28.3.0401.

Wells, M. L., and E. D. Goldberg (1992), Marine submicron particles, *Mar. Chem.*, *40*, 5–18, doi:10.1016/0304-4203(92)90045-C.

Wheeler, J. R. (1975), Formation and collapse of surface films, *Limnol. Oceanogr.*, *20*, 338–342, doi:10.4319/lo.1975.20.3.0338.

Williams, P. M. (1967), Sea surface chemistry: Organic carbon and organic and inorganic nitrogen and phosphorus in surface films and subsurface waters, *Deep Sea Res. Oceanogr. Abstr.*, *14*, 791–800.

Wurl, O., and M. Holmes (2008), The gelatinous nature of the sea-surface microlayer, *Mar. Chem.*, *110*, 89–97, doi:10.1016/j.marchem.2008.02.009.

Wurl, O., L. Miller, R. Röttgers, and S. Vagle (2009), The distribution and fate of surface-active substances in the sea-surface microlayer and water column, *Mar. Chem.*, *115*, 1–9, doi:10.1016/j.marchem.2009.04.007.

Wurl, O., E. Wurl, K. Johnson, L. Miller, and S. Vagle (2011), Formation and global distribution of sea-surface microlayers, *Biogeosciences*, *8*, 121–135, doi:10.5194/bg-8-121-2011.

Young, L. Y. (1977), Bacterioneuston examined with critical point drying and transmission electron microscopy, *Microb. Ecol.*, *4*(3), 267–277, doi:10.1007/BF02015083.

Zhang, Z., W. Cai, L. Liu, C. Liu, and F. Chen (2003), Direct determination of thickness of sea surface microlayer using a pH microelectrode at original location, *Sci. China, Ser. B: Chem.*, *46*, 339–351, doi:10.1360/02yb0192.

Zhou, J., K. Mopper, and U. Passow (1998), The role of surface-active carbohydrates in the formation of transparent exopolymer particles by bubble adsorption of seawater, *Limnol. Oceanogr.*, *43*(8), 1860–1871.

L. Miller and S. Vagle, Institute of Ocean Sciences, Fisheries and Oceans Canada, Sidney, BC V8L 4B2, Canada.

O. Wurl, Department of Ocean, Earth, and Atmospheric Sciences, Old Dominion University, Norfolk, VA 23529, USA. (owurl_nautilus@inbox.com)